THE JOURNAL OF BIOLOGICAL CHEMISTRY VOL. 287, NO. 8, pp. 6025–6034, February 17, 2012

Functional RNA Interference (RNAi) Screen Identifies System A Neutral Amino Acid Transporter 2 (SNAT2) as a Mediator of Arsenic-induced Endoplasmic Reticulum Stress*[S]

Received for publication, October 6, 2011, and in revised form, December 16, 2011 Published, JBC Papers in Press, January 3, 2012, DOI 10.1074/jbc.M111.311217

Raymond S. Oh[‡§¶], Wen-Chi Pan[‡§], Abdullah Yalcin[¶], Hong Zhang[‖], Tomás R. Guilarte[**], Gökhan S. Hotamisligil[¶], David C. Christiani[§], and Quan Lu[‡§¶1]

*From the [‡]Program in Molecular and Integrative Physiological Sciences, the [§]Department of Environmental Health, and the [¶]Department of Genetics and Complex Diseases, Harvard School of Public Health, Boston, Massachusetts 02115, the [‖]Department of Cell Biology, University of Massachusetts Medical School, Worcester, Massachusetts 01655, and the **Department of Environmental Health Sciences, Mailman School of Public Health, Columbia University, New York, New York 10032*

Background: Arsenic causes ER stress, but the underlying mechanisms remain incompletely understood.
Results: A genome-wide RNAi screen identifies human genes that mediate arsenite-induced ER stress.
Conclusion: Up-regulation of the amino acid transporter SNAT2 links mTOR activation and ER stress during arsenite exposure.
Significance: Our study helps to better understand arsenic-related human diseases, such as cancer and diabetes.

Exposure to the toxic metalloid arsenic is associated with diabetes and cancer and causes proteotoxicity and endoplasmic reticulum (ER) stress at the cellular level. Adaptive responses to ER stress are implicated in cancer and diabetes; thus, understanding mechanisms of arsenic-induced ER stress may offer insights into pathogenesis. Here, we identify genes required for arsenite-induced ER stress response in a genome-wide RNAi screen. Using an shRNA library targeting ~20,000 human genes, together with an ER stress cell model, we performed flow cytometry-based cell sorting to isolate cells with defective response to arsenite. Our screen discovered several genes modulating arsenite-induced ER stress, including sodium-dependent neutral amino acid transporter, SNAT2. SNAT2 expression and activity are up-regulated by arsenite, in a manner dependent on activating transcription factor 4 (ATF4), an important mediator of the integrated stress response. Inhibition of SNAT2 expression or activity or deprivation of its primary substrate, glutamine, specifically suppressed ER stress induced by arsenite but not tunicamycin. Induction of SNAT2 is coincident with the activation of the nutrient-sensing mammalian target of rapamycin (mTOR) pathway, which is at least partially required for arsenite-induced ER stress. Importantly, inhibition of the SNAT2 or the System L transporter, LAT1, suppressed mTOR activation by arsenite, supporting a role for these transporters in modulating amino acid signaling. These findings reveal SNAT2 as an important and specific mediator of arsenic-induced ER stress, and suggest a role for aberrant mTOR activation in arsenic-related human diseases. Furthermore, this study demonstrates the utility of RNAi screens in elucidating cellular mechanisms of environmental toxins.

Arsenic contamination in the environment poses a major threat to global public health. Epidemiological studies observe a link between arsenic exposure, primarily via contaminated drinking water, and the development of numerous chronic diseases, such as cancer, type 2 diabetes, and cardiovascular disease (reviewed in Refs. 1–3). The precise molecular mechanisms leading to arsenic toxicity and disease development are not well understood. Arsenite (As(III)), a toxic inorganic species found in ground water, can react with thiols, resulting in protein damage and oxidative stress (4). Consequently, arsenite elicits stress responses that counteract protein misfolding, such as induction of heat shock protein chaperones (5), ubiquitin-proteasome system components (6), and the unfolded protein response (UPR)[2] (7–11).

Various stresses (*e.g.* glucose deprivation and oxidative stress) can disrupt endoplasmic reticulum (ER) function, leading to the accumulation of misfolded proteins in the organelle, inducing a condition called ER stress (12). To maintain organelle homeostasis, an adaptive transcriptional response program, the UPR, expands ER functional capacities, such as chaperoning and degradation, and promotes recovery from stress via the integrated stress response (reviewed in Ref. 13). Mammalian UPR is initiated by ER-localized membrane proteins, inositol-requiring protein 1 (IRE1), activating transcription factor 6 (ATF6), and PKR-like ER kinase (PERK); these proteins regulate three canonical branches of the UPR. During ER stress,

* This work was supported, in whole or in part, by National Institutes of Health, Harvard-NIEHS Center, Grant P30ES000002 and NIEHS Superfund Research Program Grant P42ES016454 (to Q. L.) and National Institutes of Health Grants DK052539 and DK090942 (to G. S. H.).
[S] This article contains supplemental Table S1 and Figs. S1–S3.
[1] To whom correspondence should be addressed: Harvard School of Public Health Bldg. I-305, 665 Huntington Ave., Boston, MA 02115. Tel.: 617-432-7145; E-mail: qlu@hsph.harvard.edu.

[2] The abbreviations used are: UPR, unfolded protein response; ER, endoplasmic reticulum; PERK, PKR-like ER kinase; mTOR, mammalian target of rapamycin; eIF-2α, eukaryotic initiation factor 2; CHOP, C/EBP-homologous protein; HEK, human embryonic kidney; FACS, fluorescence-activated cell sorting; MeAIB, (methylamino)isobutyric acid; S6K1, p70-ribosomal S6 kinase; BCH, 2-aminobicyclo-(2,2,1)-heptanecarboxylic acid; qPCR, quantitative real-time RT-PCR.

the endoribonuclease function of IRE1 splices X-box-binding protein 1 (*XBP1*) mRNA, resulting in translation of this UPR-promoting transcription factor (14). ATF6 translocates to the nucleus during ER stress to induce expression of ER chaperones, such as GRP78 (15). PERK is an eIF-2α kinase that promotes translation of activating transcription factor 4 (ATF4) and the integrated stress response (16, 17). UPR can also promote cell death through activation of multiple proapoptotic effectors, such as proinflammatory JNK and C/EBP-homologous protein (CHOP) (reviewed in Refs. 18 and 19).

There is growing evidence that arsenic can cause ER stress. Arsenite has been shown to activate various UPR proteins, including IRE1, GRP78, ATF4, and CHOP (7–11). The eIF-2α kinase engaged during arsenite stress is HRI or PKR (20, 21) and not PERK, indicating a non-canonical mechanism of ER stress induction. Because chronic ER stress is recognized as a factor in numerous diseases, most notably diabetes (19, 22, 23) and cancer (24, 25), it is likely that ER stress and UPR activation are important contributing factors in arsenic-associated diseases. To identify the molecular machinery involved in sensing arsenic stress and engaging ER stress response pathways, we performed a genome-wide RNAi screen for genes required for arsenite-induced ER stress. One of the validated RNAi hits is sodium-dependent neutral amino acid transporter 2 (SNAT2), which is activated by arsenite stress in an ATF4-dependent manner. This arsenite-induced increase in SNAT2 activity appears to link mTOR activity and ER stress during exposure to this toxin.

EXPERIMENTAL PROCEDURES

Cell Culture and Chemicals—Human embryonic kidney HEK293 and HEK293T cells were cultured as previously described (26). Mouse 3T3L1 adipocytes were cultured and differentiated as described previously (27). Experiments on adipocytes were performed on days 8–10 after starting differentiation. All chemicals were obtained from Sigma-Aldrich.

CHOP Promoter Reporter Construct and Cell Line Generation, Lentiviral shRNA Library, and Screening—A human *CHOP* promoter construct was a gift from P. Fafournoux (28). The promoter region (−649 to +91) was extended at the 3′-end to include the complete upstream ORF that inhibits basal *CHOP* expression (29). The 3′-end was extended using two overlapping primers (5′- GTATGAAGATACACTTCCTTCT-TGAACACTCTCTCCTCAGGTTCCAGCT-3′ and 5′-CGG-GATCCCGTCAGGTGTGGTGATGTATGAAGATACACT-TCCTTC-3′) in sequential PCRs by standard procedures (30). This promoter region (−649 to +136) DNA fragment was cleaved with XhoI and HindIII restriction enzymes (New England BioLabs) and cloned into the mCherry fluorescent protein construct (pmCherry-1, Clontech). HEK293 cells were then transfected with the reporter construct using Turbofect reagent, according to the manufacturer's instructions (Fermentas), and clones resistant to G418 antibiotic (500 μg/ml) were generated. Several clones were characterized for reporter induction by arsenite by fluorescence-activated cell sorting (FACS), and one was selected for further study.

A genome-wide shRNA library (GIPZ Lentiviral shRNAmir, V2L, Open Biosystems) was used in the study. To generate pooled viral particles, HEK293T cells were transfected with shRNA vector library pools and HIV-1-based packaging and envelope gene constructs. A negative "non-silencing" shRNA control was also prepared in this manner. Collection and titering of virus was performed according to Open Biosystems protocols. Approximately 2×10^7 CHOP reporter HEK293 cells were then transduced with the viral library, and $\sim 6 \times 10^6$ cells were successfully infected, according to expression of a GFP marker present on the shRNA vector. Stable vector integration was obtained with puromycin selection.

Approximately 5×10^7 shRNA library cells or negative control shRNA-transduced reporter cells were treated with arsenite and collected by trypsinization, and then $\sim 5 \times 10^6$ dim mCherry-expressing cells were isolated by FACS (BD FACSAria II). Isolated cells were replated, and after 10–14 days of growth, arsenite treatment and FACS were repeated. After four cycles of treatment and FACS, genomic DNA was extracted (Gentra Puregene, Qiagen). The shRNA cassette was amplified by PCR with vector primers and subcloned into the library vector by standard methods (30). This "sublibrary" of shRNAs was then transformed into supercompetent *Escherichia coli* (Stratagene), which produced $\sim 5 \times 10^4$ individual bacterial colonies. shRNA plasmid was recovered from 268 clones and sequenced using vector sequencing primers. Target gene identity was determined with the genome search engine, BLAT (University of California, Santa Cruz) (31).

Flow Cytometry Assay—To evaluate the reporter phenotype produced by individual shRNAs, CHOP reporter cells were transduced with individual lentiviral shRNA particles. Lentiviral particles were prepared and shRNA-transduced into the reporter cell line as described above. Following puromycin selection, cells were treated with arsenite (15 μM, 16 h) and then analyzed by flow cytometry (BD LSRII). All flow cytometry data were collected using BD Diva software and analyzed with DeNovo FCS Express software.

siRNA Transfections—HEK293T cells were transfected with 100 nM siRNA (Sigma) (guide strands, 5′-AUUGGCACAG-CAUAGACAG (si1) or 5′-ACUAUGAAGAGGUAGCUUG (si2)) targeting *SNAT2* mRNA (accession NM_018976). Cells were also transfected with siRNA (Sigma) (guide strand, 5′-AAUCUGUCCCGGAGAAGGC, targeting *ATF4* mRNA (accession NM_001675)) or non-targeting siRNA control (Sigma, Mission Universal Negative Control 1), using Dharmafect 1 transfection reagent (Dharmacon), according to the manufacturer's instructions. Cells were treated 48 h after transfection with stressor.

Quantitative Real-time RT-PCR Analysis—Following experimental treatments of cells, RNA was extracted and column-purified (Qiagen), and cDNA was generated by reverse transcription (Invitrogen). Quantitative real-time RT-PCR (qPCR) analysis was performed using Quantitect SYBR Green reagent (Qiagen) on a 7300 real-time PCR system (ABI). Relative gene expression was determined using the $\Delta\Delta CT$ method, using β-actin as internal control. Primer specificity was confirmed by melting curve analysis. PCR primer sequences are provided in supplemental Table 1.

Immunoblot Analysis—Following experimental treatments, cells were washed with PBS and lysed in ice-cold radioimmu-

noprecipitation buffer, supplemented with protease inhibitors and phosphatase inhibitors (Roche Applied Science). Lysates were precleared by centrifugation, and then 20 μg of total protein was separated by SDS-PAGE electrophoresis (NuPAGE, Invitrogen) and transferred onto nitrocellulose (Hybond ECL, Amersham Biosciences). Subsequent immunoblotting and detection of enhanced chemiluminescence reaction by horseradish peroxidase were performed by standard methods. Antibodies used were as follows: anti-CHOP (for human CHOP detection) and ATF4 from Genetex; anti-CHOP (for mouse CHOP detection) and β-actin from Santa Cruz Biotechnology, Inc. (Santa Cruz, CA); anti-SNAT2/SLC38A2 from AbCam; and anti-phospho-Thr-389 and total S6K1 and phospho-Ser-473 and total AKT antibodies from Cell Signaling. For immunoblot quantitation, chemiluminescence was captured with an Alpha Innotech Fluorchem Imager and analyzed with AlphaEaseFC software.

2-(Methylamino)isobutyric Acid (MeAIB) Uptake Assay—3T3L1 adipocytes cultured in 24-well plates were serum-starved for 16 h and then treated with various stressors in serum-free medium. For HEK293T, cells were seeded on poly-L-lysine 24-well plates and transfected with siRNAs. After 2 days, cells were serum-starved for 16 h and then treated with arsenite. Following stress treatments, cells were washed with Hepes-buffered saline (pH 7.7) and then incubated in 17 μM [^{14}C]MeAIB (PerkinElmer Life Sciences), for 10 min at room temperature. Cells were then washed twice with cold Hepes-buffered saline and then lysed in 1% SDS, 50 mM sodium hydroxide. Equal protein quantities were mixed with scintillant, and radioactivity was measured. To determine specific System A uptake of [^{14}C]MeAIB, the radioactive count measured from cells co-treated with competitive cold MeAIB (10 mM) was subtracted from all sample counts.

Statistical Analysis—Student's *t* test with two tails was calculated where indicated in the figure legends. $p \leq 0.05$ was considered significant. On bar charts, *error bars* indicate S.E. values. Statistics were calculated with GraphPad Prism software.

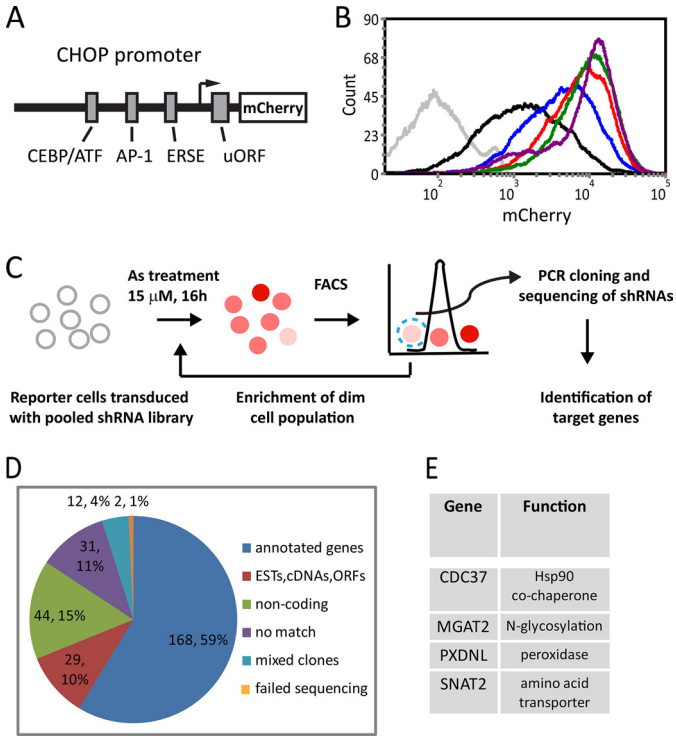

FIGURE 1. **Genome-wide shRNA screen identifies genes required for arsenite-induced ER stress.** *A*, *CHOP* promoter mCherry reporter construct. A human *CHOP* promoter fragment containing the CEBP-ATF composite site, AP-1 site, and ERSE element, which are involved in arsenite and ER stress induction of *CHOP* (64–66), was used to drive fluorescent mCherry expression. *B*, dose-dependent mCherry induction in a clonal HEK293 stable reporter cell line. Cells were treated with arsenite (5 μM (*blue*), 15 μM (*red*), or 30 μM (*green*)) or tunicamycin (5 μg/ml (*purple*)) for 16 h or left untreated (*black*) and then analyzed by FACS. *Silver*, control cells with no reporter. *C*, scheme of screen for genes required for reporter induction. Pools of shRNA lentivirus were stably transduced into the reporter cell line. Following arsenite treatment, weak activators were isolated by FACS, which were then regrown and subjected to further rounds of induction and FACS for enrichment of this "weak activator" cell population. shRNAs from this population were PCR-cloned and sequenced to identify target genes. *D*, primary screen results. Sequencing of 268 shRNA clones identified 168 annotated genes, which were selected for further analysis (for details, see "Results"). *E*, gene hits validated by shRNA and siRNA. Genes whose knockdown by shRNA and siRNA reduced arsenite-induced reporter activity or endogenous *CHOP* expression, respectively, were considered validated.

RESULTS

Genome-wide shRNA Screen Identifies Genes Required for Arsenite-induced ER Stress—We performed a FACS-based shRNA screen, assaying transcriptional activation of *CHOP* as a read-out of ER stress. *CHOP*, a member of the C/EBP family of transcription factors, is activated by PERK-ATF4, ATF6, and IRE1 (15, 32, 33) and thus receives positive inputs from all major UPR pathways. A transgene reporter encoding mCherry under control of the *CHOP* promoter was constructed (Fig. 1*A*) and stably introduced into HEK293 cells. This reporter demonstrated responsiveness to both arsenite and the classic ER stressor, tunicamycin (Fig. 1*B*). Induction of the reporter was dose-dependent, and treatment with 15 μM arsenite produced a ~10-fold increase in mean mCherry fluorescence and caused minimal cell toxicity (supplemental Fig. S1*A*).

A genome-wide lentiviral shRNA library, containing 65,000 shRNAs targeting ~20,000 human genes, was used in this study. The stable HEK293 reporter cells were transduced with the lentiviral shRNA library at a relatively low multiplicity of infection (0.3) to avoid multiple transductions per cell. The final cell population contained ~6 million independent viral integration events, providing ~90-fold coverage of the shRNA library. To identify genes required for arsenite-induced *CHOP* expression, reporter cells transduced with the shRNA library were first treated with arsenite (15 μM, 16 h) to activate the reporter. Cells with weak mCherry induction, presumably due to shRNA-mediated knockdown of *CHOP* "activators," were isolated by FACS (Fig. 1*C*). Cells isolated by this procedure were allowed to repopulate and subjected to four additional rounds of arsenite induction and FACS to enrich for the "weak responder" population. From this final population, genomic DNA was recovered, and 268 shRNAs were sequenced, of which 59% targeted annotated genes (Fig. 1*D*). Hits were prioritized by frequency of occurrence, with 17 genes identified two or more times.

From this primary screen, we identified IRE1, which demonstrated that the screen was capable of identifying established ER stress modulators. The 17 primary screen hits were subjected to secondary screening, where the suppressive effect of individual

shRNAs on reporter induction was evaluated. Additionally, because of potential off-target shRNA effects, the ability of unique siRNAs to suppress endogenous *CHOP* induction in transfected HEK293T cells was examined. Four genes passed validation by these two methods and are listed in Fig. 1*E* and supplemental Fig. S1, *B* and *C*). Although the effect of single gene knockdowns on *CHOP* induction was modest, it was not unexpected because *CHOP* expression is controlled by multiple redundant UPR signaling pathways (15, 32, 33). Furthermore, the effect of siRNA and shRNA on target gene expression was itself modest, achieving ~40–60% knockdown in most cases (supplemental Fig. S1*D*).

Among the validated gene hits, CDC37 is an Hsp90 co-chaperone that is essential for the maturation of eIF-2α kinases HRI and GCN2 (34, 35). Indeed, Hsp90 is required for activation of IRE1, ATF6, and PERK branches of the UPR, as revealed by a recently developed specific Hsp90 inhibitor (36). MGAT2 is a Golgi-localized glycosyltransferase, which is up-regulated during plasma cell differentiation by XBP1 (37). PXDNL is a putative secreted peroxidase (38). SNAT2 is the most broadly expressed subtype of three System A transporters that mediate sodium-coupled uptake of small, aliphatic amino acids, such as glutamine, alanine, and cysteine (39).

Reduced SNAT2 Expression, Inhibition of Transporter Activity, or Glutamine Deprivation Suppresses Arsenite-induced ER Stress—There is a growing appreciation that cellular nutrient abundance is intimately tied to endoplasmic reticulum function (40). Because SNAT2 is an amino acid transporter that displays regulated expression (*e.g.* in response to amino acid deprivation and hyperosmotic stress (41, 42)), we further examined its role in arsenite-induced ER stress. Two different *SNAT2* siRNAs suppressed arsenite-induced endogenous *CHOP* expression compared with control (~60% for siRNA 1, 80% for siRNA 2), as assessed by qPCR (Fig. 2*A*). This effect was achieved with ~60% (siRNA 1) or 45% (siRNA 2) *SNAT2* knockdown efficiency. Induction of CHOP protein levels was also significantly suppressed with *SNAT2* siRNA (~50% of control) (Fig. 2*D*). Interestingly, we observed ~3-fold induction of *SNAT2* itself by arsenite, which could be inhibited by *SNAT2* siRNAs (Fig. 2*A*). Importantly, we also observed that *SNAT2* siRNAs could reduce the amount of spliced *XBP1* induced by arsenite (~50% for siRNA 1, 67% for siRNA 2) (Fig. 2*B*). Splicing of *XBP1* is another indicator of ER stress. Thus, the role of SNAT2 in arsenite response is not limited to CHOP induction but broadly affects the UPR. However, *SNAT2* siRNAs do not have a significant suppressive effect on tunicamycin-induced *CHOP* (Fig. 2*C*), suggesting a specific role for SNAT2 in the arsenite response.

We next asked whether inhibition of SNAT2 transporter activity could suppress arsenite-induced ER stress. The amino acid analog MeAIB is a specific substrate of System A transporters that inhibits transporter activity at saturating concentrations (39). We examined the effect of MeAIB on arsenite-treated 3T3L1 adipocytes, which are commonly used in studies of ER stress due to their high metabolic activity. Treatment of adipocytes with 10 mM MeAIB for 3 h can reduce System A activity to ~30% (uptake assay; Fig. 3*D*). MeAIB suppressed CHOP induction by arsenite (~60% of control) (Fig. 2, *E* and *G*). Treatment with MeAIB also suppressed induction of GRP78 (~67% of control), another read-out of UPR activation (15) (Fig. 2*F*). We attribute the effect of MeAIB on 3T3L1 adipocytes to be mainly due to inhibition of SNAT2 because basal as well as arsenite-induced expression of other System A transporters is relatively low in this cell line (supplemental Fig. S2*A*).

Next, we determined whether the amino acids transported by SNAT2 mediate its effect on arsenic-induced ER stress. Glutamine is a SNAT2 substrate of particular importance because it is the most abundant free amino acid in plasma and in cell culture medium and is vital for cell metabolism and protein synthesis (43). Pretreatment with glutamine-free medium (3 h) suppressed arsenite induction of CHOP (~75% of control RNA, ~50% of control protein) and *GRP78* (~62% of control) (Fig. 2, *E–G*). MeAIB treatment and glutamine starvation could not dampen significantly tunicamycin-induced *CHOP* or *GRP78* (supplemental Fig. S2*B*). These data indicate that arsenite-induced ER stress and UPR require, at least in part, SNAT2-mediated amino acid transport.

SNAT2 Expression and Activity Is Induced by Arsenite in an ATF4-dependent Manner—As observed in HEK293T cells (Fig. 2*A*), *SNAT2* expression is inducible by arsenite treatment. SNAT2 expression is also arsenite-inducible in 3T3L1 adipocytes, in a dose- and time-dependent manner (Fig. 3*A*). Treatment with 50 μM arsenite for up to 24 h produced a steady increase in SNAT2 protein. Gene expression increased by 2-fold at 4 h, which tapers slightly at 24 h. Increasing amounts of arsenite (2–50 μM) produced steady increases in SNAT2 expression, which appears refractory at 50 μM (16 h) (Fig. 3*B*). The relative induction of SNAT2 protein appears greater than *SNAT2* mRNA, which may be due to cap-independent translation of the mRNA allowed by the 5′-UTR IRES that was reported previously (44). ER stress conditions induced by tunicamycin or another ER stressor, thapsigargin, did not increase SNAT2 protein levels (Fig. 3*C*), supporting a specific role for SNAT2 in the arsenite response.

The effect of arsenite on SNAT2 transporter activity was examined next. Uptake of radiolabeled MeAIB increased in a dose-dependent manner, increasing 2–3.5-fold at arsenite concentrations of 2–50 μM (Fig. 3*D*); a similar increase was stimulated by insulin, a known System A activator (39). No increase in uptake was seen with tunicamycin or thapsigargin, consistent with unchanging protein levels (Fig. 3*C*). A time course study revealed a steady increase in MeAIB uptake from 3 to 24 h of arsenite (50 μM) treatment (Fig. 3*E*). The dose response and time course of transporter activity are consistent with the induction pattern of SNAT2 protein (Fig. 3, *A* and *B*). *SNAT2*-targeting siRNA reduced base-line uptake (~40% of control) and abolished arsenite-stimulated uptake (Fig. 3*H*), indicating a primary role for this transporter. The induction of System A transporter activity by arsenite in our system is consistent with a previous study that demonstrated arsenite induction of System A activity in skeletal muscle cells (45).

We sought to elucidate the upstream signals controlling *SNAT2* expression during arsenite treatment. Inhibition of oxidative stress by the reactive oxygen species scavenger, *N*-acetyl cysteine (*NAC*), and mitigation of protein misfolding by a chemical chaperone, 4-phenylbutyric acid (*4PBA*), both

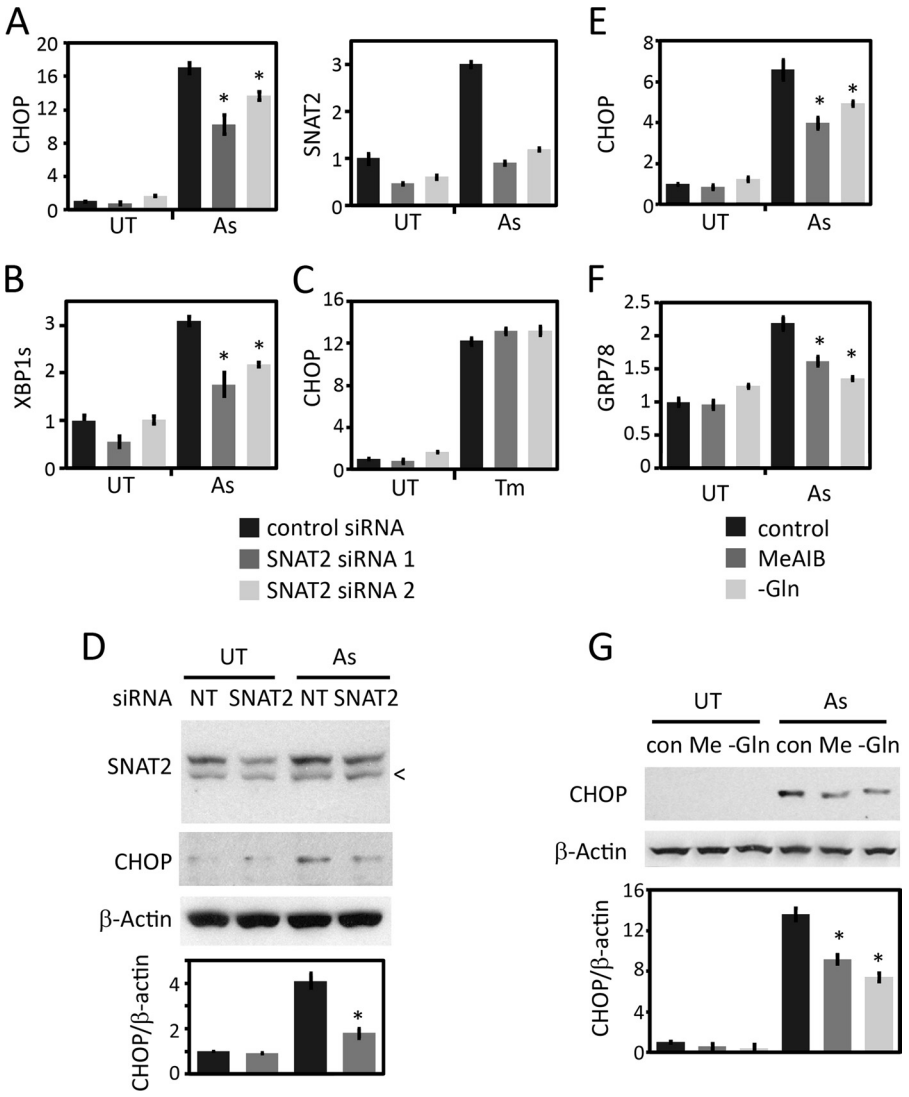

FIGURE 2. **Reduced SNAT2 expression, inhibition of transporter activity, or glutamine deprivation suppresses arsenite-induced ER stress.** *A* and *B*, *SNAT2*-targeting siRNA suppresses arsenite induction of endogenous *CHOP* and spliced *XBP1* in HEK293T cells. Gene expression levels were analyzed by qPCR. Cells were untreated (*UT*) or treated with arsenite (*As*) (15 μM, 4 h). *C*, *SNAT2*-targeting siRNAs cannot suppress tunicamycin-induced *CHOP*. Cells were treated as in *A* but with tunicamycin (*Tm*) (5 ng/ml, 4 h). $n = 2$. *D*, *SNAT2*-targeting siRNA suppresses arsenite induction of CHOP protein. Cells were treated as in *A*. CHOP protein levels were analyzed by immunoblot and normalized to β-actin. Immunoblot analysis of SNAT2 protein levels confirmed *SNAT2* knockdown. The *arrowhead* indicates a nonspecific band. *, $p < 0.01$ relative to arsenite-treated control. $n = 3$. *E–G*, inhibition of SNAT2 with saturating MeAIB (10 mM) or glutamine deprivation suppresses arsenite induction of *CHOP* and *GRP78* in 3T3L1 adipocytes. Gene expression levels were analyzed by qPCR, *E* and *F*, CHOP protein levels were analyzed by immunoblot. *G*, cells were pretreated with MeAIB or glutamine-free medium for 3 h and then co-treated with arsenite (50 μM, 4 h). *, $p < 0.01$ relative to arsenite-treated control. $n = 3$. *Error bars*, S.E.

blocked arsenite-induced *SNAT2* (Fig. 3*F*). This suggests that both oxidative stress and proteotoxic signals contribute to *SNAT2* up-regulation by arsenite. ATF4 is a key transcription factor that coordinates amino acid metabolism during amino acid starvation, ER stress, and oxidative stress (17). Arsenite can induce eIF-2α phosphorylation, resulting in increased ATF4 protein levels (10, 11), and during amino acid starvation, ATF4 binds to an amino acid response element in the *SNAT2* gene (46), suggesting a potential role in arsenite induction of *SNAT2*. Indeed, *ATF4*-targeting siRNA significantly suppressed arsenite-induced SNAT2 expression and System A activity (Fig. 3, *G* and *H*). Basal levels of SNAT2 expression and System A activity are, however, unchanged. Together, these data demonstrate that SNAT2 is part of an arsenite stress response and that up-regulation of SNAT2 by arsenite is dependent on the stress-responsive transcription factor ATF4.

mTOR Activation Links SNAT2 Activity and Arsenite-induced ER Stress—The data presented so far indicate that up-regulation of SNAT2 expression and transporter activity contribute to arsenite-induced ER stress. How might this occur? Activation of mTOR signaling is highly responsive to intracellular amino acid levels (47). A critical role for glutamine as a limiting nutrient in mTOR activation has recently been described (48), and indeed, depletion of intracellular glutamine through inhibition of SNAT2 dampens mTOR activity in muscle cells (49). mTOR is a key regulator of cell growth and promotes protein synthesis (50). An overabundance of nutrients and elevated mTOR signaling can cause ER stress (22, 51).

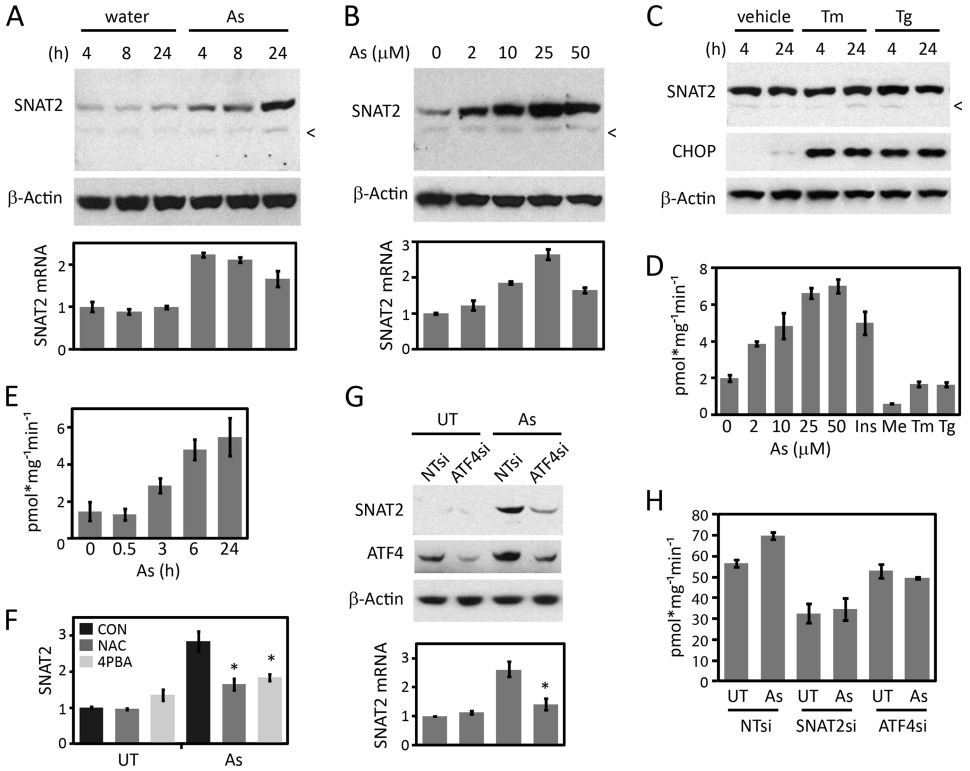

FIGURE 3. **SNAT2 expression and activity is induced by arsenite in an ATF4-dependent manner.** *A* and *B*, arsenite induces SNAT2 expression. 3T3L1 adipocytes were treated with arsenite (50 μM) or water for the times indicated (*A*) or with arsenite (16 h) at the concentrations indicated (*B*). SNAT2 Western blot (*top*) and qPCR analysis (*bottom*) ($n = 2$). The *arrowhead* denotes a nonspecific band. *C*, other forms of ER stress do not induce SNAT2 protein levels. 3T3L1 adipocytes were treated with tunicamycin (*Tm*) (5 μg/ml) or thapsigargin (*Tg*) (0.5 μM) or DMSO for the times indicated. CHOP induction demonstrates ER stress activation by these stressors. *D*, arsenite increases [^{14}C]MeAIB uptake. 3T3L1 adipocytes were treated with various stimuli, and then uptake was measured. Cells were treated with arsenite (6 h) at the indicated concentrations. Tunicamycin (5 μg/ml, 6 h) and thapsigargin (0.5 μM, 6 h) do not increase uptake. Insulin (*Ins*) (100 ng/ml, 1.5 h) is a positive control. Preincubation with saturating cold MeAIB (*Me*) (10 mM, 3 h) inhibits uptake. $n = 3$. *E*, arsenite stimulates a sustained increase in [^{14}C]MeAIB uptake. 3T3L1 adipocytes were treated with arsenite (50 μM) for up to 24 h, and then the uptake assay was performed. $n = 3$. *F*, *N*-acetyl cysteine (*NAC*) or 4-phenylbutyric acid (*4PBA*) inhibits arsenite induction of *SNAT2*. 3T3L1 adipocytes were pretreated with *N*-acetyl cysteine (10 mM), 4-phenylbutyric acid (10 mM), or water (*con*) for 30 min and then co-treated with arsenite (50 μM, 6 h). *SNAT2* expression was analyzed by qPCR. *, $p < 0.05$ relative to arsenite-treated control. $n = 2$. *UT*, untreated. *G*, *ATF4*-targeting siRNA blunts SNAT2 induction by arsenite. SNAT2 expression was analyzed by qPCR (*bottom*) and immunoblot analysis (*top*). ATF4 Western blot demonstrates knockdown. HEK293T cells were untreated or treated with arsenite (15 μM, 16 h). *, $p = 0.01$ relative to arsenite-treated NTsi control. $n = 3$. *H*, *SNAT2*- and *ATF4*-targeting siRNAs inhibit arsenite-induced [^{14}C]MeAIB uptake. HEK293T cells were untreated or treated with arsenite (15 μM, 4 h), and then the uptake assay was performed. $n = 3$. *Error bars*, S.E.

Thus, we hypothesized that arsenite might contribute to ER stress through SNAT2 induction, leading to enhanced mTOR signaling.

As a read-out of mTOR signaling, we examined the phosphorylation of S6K1 on Thr-389. S6K1 is a direct substrate of the mTOR kinase within mTOR complex 1 (mTORC1). Cells were serum-starved overnight to reduce basal mTOR activity and then treated with arsenite. Arsenite increased S6K1 phosphorylation in a dose- and time-dependent manner in both 3T3L1 adipocytes and HEK293T cells (Fig. 4, *A* and *B*, and supplemental Fig. S3, *A* and *B*). Increases in S6K1 phosphorylation were apparent from 1.5 to 6 h of arsenite treatment (50 μM), and from 2 to 50 μM (6 h). Importantly, the latency, response time, and dose response of S6K1 phosphorylation are coincident with System A induction (Fig. 3, *D* and *E*). Increased S6K1 phosphorylation was completely blocked by rapamycin, confirming that this reflects increased mTOR signaling. However, arsenite did not stimulate AKT phosphorylation, indicating that mTOR activation by arsenite does not involve this upstream pathway.

We next examined whether increased mTOR activity contributes to arsenite-induced ER stress. Inhibition of mTORC1 by rapamycin suppressed arsenite-induced CHOP expression in 3T3L1 adipocytes (~10% compared with control) (Fig. 4*C*). Rapamycin treatments in HEK293T cells also reduced CHOP induction (~50% of control) and *XBP1* splicing (~60% of control) (Fig. 4*D* and supplemental Fig. S3*C*). Therefore, mTOR activity is activated by arsenite and contributes to arsenite-induced ER stress.

To test whether SNAT2 contributes to mTOR activation by arsenite, siRNA knockdown of SNAT2 was performed. Compared with non-targeting control, *SNAT2*-targeting siRNA reduced phosphorylated S6K1 levels induced by arsenite (~60% of control) (Fig. 4*E*). The effect of SNAT2 inhibition was also tested. MeAIB co-treatments significantly reduced arsenite-induced S6K1 phosphorylation (Fig. 4*F*). We attribute the effect of MeAIB mainly to inhibition of SNAT2 and possibly SNAT1, whose expression is abundant and modestly inducible by arsenite in HEK293T cells (supplemental Fig. S3*D*). Glutamine starvation also blunted arsenite-stimulated S6K1 phosphorylation (Fig. 4*F*), indicating the importance of glutamine availability.

System L transporters couple the efflux of intracellular glutamine to the import of large branched amino acids, which are the most potent mTOR activation amino acids (48, 52, 53).

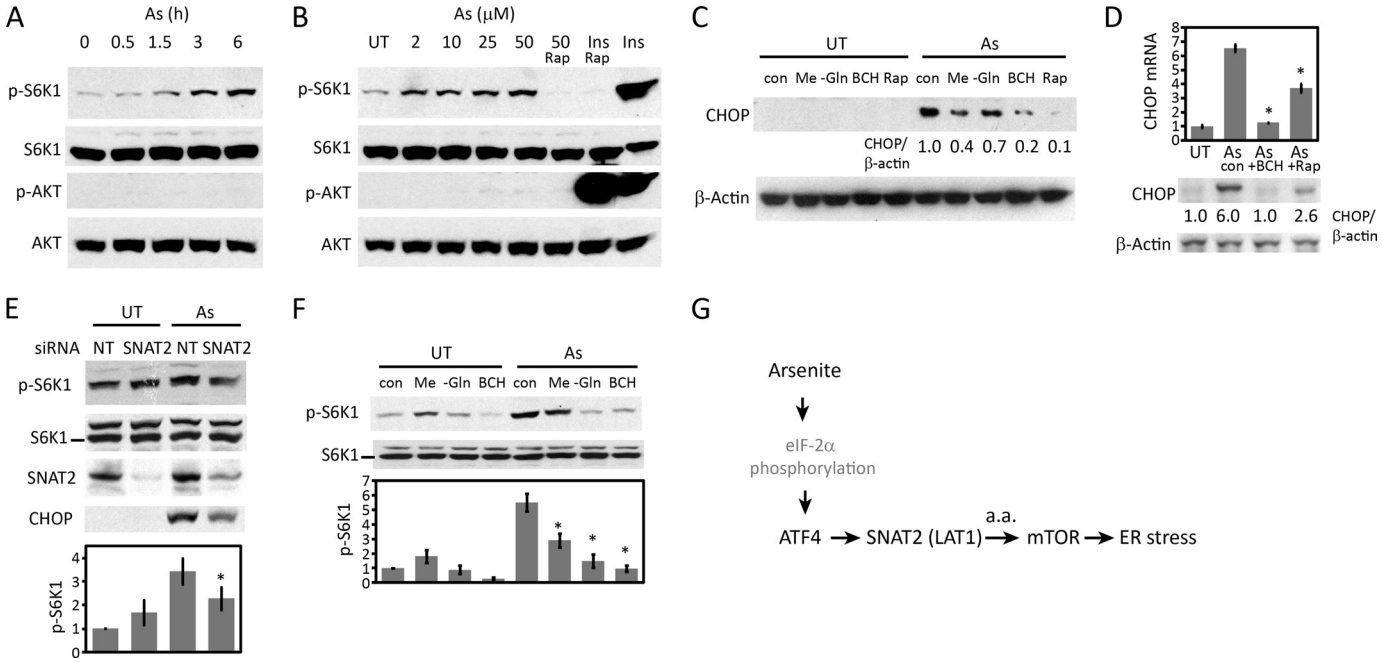

FIGURE 4. **mTOR activation links SNAT2 activity and arsenite-induced ER stress.** *A* and *B*, arsenite induces S6K1 phosphorylation. 3T3L1 adipocytes were serum-starved (16 h) and then treated with arsenite (50 μM) for the times indicated. *A*, arsenite induction of S6K1 phosphorylation is dose-responsive and rapamycin-sensitive. *B*, starved 3T3L1 adipocytes were treated with arsenite at the concentrations indicated for 6 h. Rapamycin (*Rap*) (20 nM, 30 min) pretreatment can inhibit S6K1 phosphorylation induced by arsenite or insulin (*Ins*) (100 nM, 90 min). Phospho-S6K1, total S6K1, phospho-AKT, and total AKT were analyzed by immunoblot. *UT*, untreated. *C*, inhibition of System A or L transport, glutamine deprivation, and rapamycin suppresses arsenite-induced CHOP. 3T3L1 adipocytes were pretreated with MeAIB (10 mM, 3 h), glutamine-free medium (3 h), BCH (10 mM, 3 h), or rapamycin (20 nM, 30 min) and then co-treated with arsenite (50 μM, 4 h). CHOP induction was analyzed by immunoblot. *D*, rapamycin or BCH (System L transport inhibitor) suppresses arsenite-induced ER stress. HEK293T cells were pretreated with rapamycin (20 nM, 30 min) or BCH (10 mM, 3 h) and then co-treated with arsenite (15 μM, 3 h). CHOP expression was analyzed by qPCR (*top*) and immunoblot. *, $p < 0.01$ relative to arsenite-treated control. $n = 3$. *E*, siRNA knockdown of SNAT2 reduces arsenite-induced S6K1 phosphorylation. HEK293T cells transfected with *SNAT2*-targeting siRNA were serum-starved (16 h) and then treated with arsenite (15 μM, 3 h). Phospho-S6K1 values were normalized to untreated, non-targeting siRNA control. *, $p < 0.05$ relative to arsenite-treated control. $n = 3$. *F*, MeAIB, BCH, or glutamine deprivation suppresses arsenite-induced S6K1 phosphorylation. Serum-starved (16 h) HEK293T cells were pretreated with MeAIB, BCH, or glutamine-free medium, as in *E*, and then co-treated with arsenite (15 μM) for 3 h. Phospho-S6K1 levels were normalized to untreated control. *, $p < 0.05$ relative to arsenite-treated control. $n = 2$. *G*, proposed model of SNAT2 activation of mTOR and ER stress during arsenite exposure. *Error bars*, S.E.

System A transporters, such as SNAT2, therefore, directly supply amino acids that drive System L function. LAT1/SLC7A5, a transporter that exchanges glutamine for leucine, can be inhibited by 2-aminobicyclo-(2,2,1)-heptanecarboxylic acid (BCH), a specific System L inhibitor (54). BCH alone inhibited S6K1 phosphorylation and blunted the arsenite response (Fig. 4*F*). Furthermore, BCH could significantly suppress CHOP expression and *XBP1* splicing induced by arsenite (Fig. 4, *C* and *D*, and supplemental Fig. S3*C*). Together, these data suggest that arsenite-induced ER stress and activation of the UPR are enhanced by SNAT2- and LAT1-mediated mTOR activation (Fig. 4*G*).

DISCUSSION

In this study, we performed a genome-wide functional RNAi screen to identify genes required for the ER stress response induced by arsenic. The data presented demonstrate, to our knowledge, the first utilization of a functional RNAi screen for ER stress activation in mammalian cells. The data also highlight the utility of RNAi screening to elucidate cellular mechanisms of environmental toxins. The screen identified several putative modulators of arsenite-induced ER stress, including genes with known functions in stress response (*CDC37*, *SNAT2*). Mechanistic studies of SNAT2 established an important role for this neutral amino acid transporter in linking arsenite exposure, mTOR activation, and ER stress.

Our findings identify SNAT2 as a novel component of the arsenite stress response. We demonstrated that SNAT2 and its transporter activity are required for arsenite-induced ER stress, as measured by induced CHOP, *XBP1* splicing, and *GRP78*. Furthermore, SNAT2 expression and activity are induced by arsenite. SNAT2 is the most broadly expressed subtype of three System A transporters that mediate sodium-coupled uptake of small, aliphatic amino acids, such as glutamine, alanine, and cysteine (39). Regulation of *SNAT2* expression by hyperosmotic stress and amino acid deprivation has previously been documented (41, 42), but this is the first demonstration of SNAT2 regulation by arsenite. We further demonstrate that arsenite induction of *SNAT2* requires ATF4 and both oxidative stress and proteotoxic upstream signals. During amino acid deprivation, SNAT2 expression can be regulated by both transcriptional activation, via ATF4 (46), and cap-independent translation of the mRNA allowed by the IRES in the 5′-UTR (44). Similar regulatory mechanisms are likely to be activated by arsenite, which can induce eIF-2α phosphorylation and ATF4 expression (10, 11). During stress conditions, ATF4-mediated induction of amino acid transporters, such as LAT1 (17) and SNAT2, may support the increased demand for protein chaperone synthesis as well as the supply of proteins and peptides involved in redox reactions (*i.e.* glutathione), therefore mitigating oxidative stress (43). Glutamine also supports glucose

metabolism (43), which is severely compromised during arsenite stress (55). Thus, several potential adaptive mechanisms are supported by SNAT2. SNAT2 activity cannot be induced by tunicamycin or thapsigargin, indicating its specificity in the arsenite response. Previous studies have shown that thapsigargin can suppress *SNAT2* expression by an unknown mechanism downstream of ATF4 recruitment (56), suggesting that ER stress may generate a repressive signal. Thus, one possible explanation for the apparent specificity in SNAT2 induction is that arsenite does not elicit an adequate repressive ER stress signal in contrast to potent ER stressors tunicamycin and thapsigargin.

Previous studies have demonstrated that arsenite can activate mTOR (57, 58), which we also observe in HEK293T and 3T3 L1 adipocytes. Multiple stresses impinge on mTOR, which maintains the appropriate balance between anabolic processes, like protein synthesis, and catabolic processes, such as autophagy. It is not clear how arsenite activates mTOR, although very recently Raptor phosphorylation by p38β has been suggested as one potential mechanism (59). Intracellular amino acid availability is recognized as a major mTORC1 regulatory mechanism (47), and recent studies have revealed an important regulatory role for glutamine transporters (48, 49, 52). Cellular import of glutamine can be regulated by at least four different transporter types (Systems A, N, ASC, and L) (60). SLC1A5 (a System ASC transporter) and SNAT2 have been shown to regulate basal mTOR activity in HeLa and muscle cells, respectively (48, 49, 52). By concentrating intracellular amino acids like glutamine, these transporters provide exchange substrates for System L transporters (LAT1) and therefore drive the import of branched amino acids like leucine, which are potent mTORC1 activators (48, 52). Our findings suggest that during arsenite stress, amino acid signaling to mTORC1 can be enhanced by elevated SNAT2 transporter activity. First, there is a temporal correlation in S6K1 phosphorylation and SNAT2 expression and System A activity. Furthermore, specific inhibition of System A, glutamine starvation, or *SNAT2*-targeting siRNA suppressed S6K1 phosphorylation. Last, inhibition of LAT1 also suppressed arsenite-induced S6K1 activation. In addition, consistent with an amino acid signaling mechanism, the PI3K/AKT pathway is not activated. These findings indicate that SNAT2 transporter activity is important for mTOR activation during arsenite stress.

During arsenite stress, SNAT2 up-regulation may promote adaptation through mTOR-dependent as well as mTOR-independent anabolic processes, as described above. However, this can lead to overloading of the ER and consequently ER stress and provides an explanation as to why inhibition or reduced expression of SNAT2 and LAT1 suppressed arsenite-induced ER stress. Previous studies have demonstrated that overactive mTOR activity can cause ER stress and activate the UPR (51), presumably due to increased protein synthesis in the ER. Consistent with this view, inhibition of mTORC1 with rapamycin in 3T3L1 adipocytes and HEK293T cells partially blocked arsenite-induced ER stress. Together, our data support a model where arsenite activation of SNAT2, in an ATF4-dependent manner, increases System A activity, which drives glutamine import. This leads to increased leucine import and mTORC1 activity and eventually ER stress (Fig. 4*G*).

Environmental arsenic exposure in human populations has been linked to type 2 diabetes and cancer (1, 2), but the underlying mechanisms are poorly understood. Our study suggests that altered mTOR signaling by SNAT2 activation may play an important role. A better understanding of SNAT2 activity under arsenic stress conditions and its role in arsenic-related diseases will require physiological animal models. Because ER stress and JNK activation play major roles in the negative feedback on insulin action and glucose metabolism (22, 51), our findings suggest that a SNAT2-mTOR-ER stress mechanism may contribute to arsenic's inhibitory effects on insulin signaling (55). Already, a role for SNAT2 in "nutritional stress" has been suggested because its expression and activity in the liver of diabetic mice is elevated (61, 62). Induction of SNAT2 activity may also play a role in arsenic-related cancers, through elevation of mTOR activity and UPR activation, which can promote tumor survival (24, 25, 63).

In addition to SNAT2, we have identified several other putative regulators of arsenic-induced ER stress response. The hits we report here represent only a partial list of new genes involved. Indeed, we note that the recovery of a relatively small number of shRNAs (268) from our screen limited our depth of discovery. Investigations that utilize "deep sequencing" technology will likely uncover additional potential modulators of arsenite-induced ER stress. Functional characterization of these genes and the already identified and validated RNAi hits will reveal more novel insights into the mechanisms involved and could inform human epidemiologic approaches. For example, guided by this gene set, epidemiologic and genetic studies may uncover relevant gene variants associated with the arsenic-related diabetogenic or carcinogenic effect in humans. Furthermore, because the ER stress response is a critical component of general environmental surveillance in cells, the molecular mechanisms uncovered by our screen may be relevant to other environmental exposures that cause ER and oxidative stress.

Acknowledgments—We thank Drs. L. Kobzik, B. Manning, and M. Wessling-Resnick for critical reading of the manuscript. We thank Dr. P. Fafournoux for providing the CHOP promoter construct and Dr. B. Manning for providing S6K1 and AKT antibodies and rapamycin.

REFERENCES

1. Rossman, T. G. (2003) Mechanism of arsenic carcinogenesis. An integrated approach. *Mutat. Res.* **533,** 37–65
2. Navas-Acien, A., Silbergeld, E. K., Pastor-Barriuso, R., and Guallar, E. (2008) Arsenic exposure and prevalence of type 2 diabetes in US adults. *JAMA* **300,** 814–822
3. States, J. C., Srivastava, S., Chen, Y., and Barchowsky, A. (2009) Arsenic and cardiovascular disease. *Toxicol. Sci.* **107,** 312–323
4. Bernstam, L., and Nriagu, J. (2000) Molecular aspects of arsenic stress. *J. Toxicol. Environ. Health B Crit. Rev.* **3,** 293–322
5. Del Razo, L. M., Quintanilla-Vega, B., Brambila-Colombres, E., Calderón-Aranda, E. S., Manno, M., and Albores, A. (2001) Stress proteins induced by arsenic. *Toxicol. Appl. Pharmacol.* **177,** 132–148
6. Stanhill, A., Haynes, C. M., Zhang, Y., Min, G., Steele, M. C., Kalinina, J., Martinez, E., Pickart, C. M., Kong, X. P., and Ron, D. (2006) An arsenite-inducible 19S regulatory particle-associated protein adapts proteasomes to proteotoxicity. *Mol Cell* **23,** 875–885

7. Lin, A. M., Chao, P. L., Fang, S. F., Chi, C. W., and Yang, C. H. (2007) Endoplasmic reticulum stress is involved in arsenite-induced oxidative injury in rat brain. *Toxicol. Appl. Pharmacol.* **224,** 138–146
8. Lu, T. H., Su, C. C., Chen, Y. W., Yang, C. Y., Wu, C. C., Hung, D. Z., Chen, C. H., Cheng, P. W., Liu, S. H., and Huang, C. F. (2011) Arsenic induces pancreatic β-cell apoptosis via the oxidative stress-regulated mitochondria-dependent and endoplasmic reticulum stress-triggered signaling pathways. *Toxicol. Lett.* **201,** 15–26
9. Jiang, H. Y., Jiang, L., and Wek, R. C. (2007) The eukaryotic initiation factor-2 kinase pathway facilitates differential GADD45a expression in response to environmental stress. *J. Biol. Chem.* **282,** 3755–3765
10. Fung, H., Liu, P., and Demple, B. (2007) ATF4-dependent oxidative induction of the DNA repair enzyme Ape1 counteracts arsenite cytotoxicity and suppresses arsenite-mediated mutagenesis. *Mol. Cell. Biol.* **27,** 8834–8847
11. Roybal, C. N., Hunsaker, L. A., Barbash, O., Vander Jagt, D. L., and Abcouwer, S. F. (2005) The oxidative stressor arsenite activates vascular endothelial growth factor mRNA transcription by an ATF4-dependent mechanism. *J. Biol. Chem.* **280,** 20331–20339
12. Rutkowski, D. T., and Kaufman, R. J. (2004) A trip to the ER. Coping with stress. *Trends Cell Biol.* **14,** 20–28
13. Schröder, M., and Kaufman, R. J. (2005) The mammalian unfolded protein response. *Annu. Rev. Biochem.* **74,** 739–789
14. Calfon, M., Zeng, H., Urano, F., Till, J. H., Hubbard, S. R., Harding, H. P., Clark, S. G., and Ron, D. (2002) IRE1 couples endoplasmic reticulum load to secretory capacity by processing the XBP-1 mRNA. *Nature* **415,** 92–96
15. Yoshida, H., Okada, T., Haze, K., Yanagi, H., Yura, T., Negishi, M., and Mori, K. (2000) ATF6 activated by proteolysis binds in the presence of NF-Y (CBF) directly to the cis-acting element responsible for the mammalian unfolded protein response. *Mol. Cell. Biol.* **20,** 6755–6767
16. Harding, H. P., Zhang, Y., and Ron, D. (1999) Protein translation and folding are coupled by an endoplasmic reticulum-resident kinase. *Nature* **397,** 271–274
17. Harding, H. P., Zhang, Y., Zeng, H., Novoa, I., Lu, P. D., Calfon, M., Sadri, N., Yun, C., Popko, B., Paules, R., Stojdl, D. F., Bell, J. C., Hettmann, T., Leiden, J. M., and Ron, D. (2003) An integrated stress response regulates amino acid metabolism and resistance to oxidative stress. *Mol. Cell* **11,** 619–633
18. Tabas, I., and Ron, D. (2011) Integrating the mechanisms of apoptosis induced by endoplasmic reticulum stress. *Nat. Cell Biol.* **13,** 184–190
19. Hotamisligil, G. S. (2010) Endoplasmic reticulum stress and the inflammatory basis of metabolic disease. *Cell* **140,** 900–917
20. Lu, L., Han, A. P., and Chen, J. J. (2001) Translation initiation control by heme-regulated eukaryotic initiation factor 2α kinase in erythroid cells under cytoplasmic stresses. *Mol. Cell. Biol.* **21,** 7971–7980
21. Patel, C. V., Handy, I., Goldsmith, T., and Patel, R. C. (2000) PACT, a stress-modulated cellular activator of interferon-induced double-stranded RNA-activated protein kinase, PKR. *J. Biol. Chem.* **275,** 37993–37998
22. Ozcan, U., Cao, Q., Yilmaz, E., Lee, A. H., Iwakoshi, N. N., Ozdelen, E., Tuncman, G., Görgün, C., Glimcher, L. H., and Hotamisligil, G. S. (2004) Endoplasmic reticulum stress links obesity, insulin action, and type 2 diabetes. *Science* **306,** 457–461
23. Ozcan, U., Yilmaz, E., Ozcan, L., Furuhashi, M., Vaillancourt, E., Smith, R. O., Görgün, C. Z., and Hotamisligil, G. S. (2006) Chemical chaperones reduce ER stress and restore glucose homeostasis in a mouse model of type 2 diabetes. *Science* **313,** 1137–1140
24. Romero-Ramirez, L., Cao, H., Nelson, D., Hammond, E., Lee, A. H., Yoshida, H., Mori, K., Glimcher, L. H., Denko, N. C., Giaccia, A. J., Le, Q. T., and Koong, A. C. (2004) XBP1 is essential for survival under hypoxic conditions and is required for tumor growth. *Cancer Res.* **64,** 5943–5947
25. Bi, M., Naczki, C., Koritzinsky, M., Fels, D., Blais, J., Hu, N., Harding, H., Novoa, I., Varia, M., Raleigh, J., Scheuner, D., Kaufman, R. J., Bell, J., Ron, D., Wouters, B. G., and Koumenis, C. (2005) ER stress-regulated translation increases tolerance to extreme hypoxia and promotes tumor growth. *EMBO J.* **24,** 3470–3481
26. Nabhan, J. F., Pan, H., and Lu, Q. (2010) Arrestin domain-containing protein 3 recruits the NEDD4 E3 ligase to mediate ubiquitination of the β2-adrenergic receptor. *EMBO Rep* **11,** 605–611
27. Xu, H., Sethi, J. K., and Hotamisligil, G. S. (1999) Transmembrane tumor necrosis factor (TNF)-α inhibits adipocyte differentiation by selectively activating TNF receptor 1. *J. Biol. Chem.* **274,** 26287–26295
28. Bruhat, A., Jousse, C., Carraro, V., Reimold, A. M., Ferrara, M., and Fafournoux, P. (2000) Amino acids control mammalian gene transcription. Activating transcription factor 2 is essential for the amino acid responsiveness of the CHOP promoter. *Mol. Cell. Biol.* **20,** 7192–7204
29. Jousse, C., Bruhat, A., Carraro, V., Urano, F., Ferrara, M., Ron, D., and Fafournoux, P. (2001) Inhibition of CHOP translation by a peptide encoded by an open reading frame localized in the chop 5′-UTR. *Nucleic Acids Res.* **29,** 4341–4351
30. Sambrook, J., and Russell, D. W. (2001) *Molecular Cloning: A Laboratory Manual*, 3rd Ed., Chapter 8, pp. 8.1–8.113, Cold Spring Harbor Laboratory Press, Cold Spring Harbor, NY
31. Kent, W. J. (2002) BLAT. The BLAST-like alignment tool. *Genome Res.* **12,** 656–664
32. Harding, H. P., Novoa, I., Zhang, Y., Zeng, H., Wek, R., Schapira, M., and Ron, D. (2000) Regulated translation initiation controls stress-induced gene expression in mammalian cells. *Mol. Cell* **6,** 1099–1108
33. Wang, X. Z., Harding, H. P., Zhang, Y., Jolicoeur, E. M., Kuroda, M., and Ron, D. (1998) Cloning of mammalian Ire1 reveals diversity in the ER stress responses. *EMBO J.* **17,** 5708–5717
34. Donzé, O., and Picard, D. (1999) Hsp90 binds and regulates Gcn2, the ligand-inducible kinase of the α subunit of eukaryotic translation initiation factor 2 [corrected]. *Mol. Cell. Biol.* **19,** 8422–8432
35. Shao, J., Grammatikakis, N., Scroggins, B. T., Uma, S., Huang, W., Chen, J. J., Hartson, S. D., and Matts, R. L. (2001) Hsp90 regulates $p50^{cdc37}$ function during the biogenesis of the activeconformation of the heme-regulated eIF2α kinase. *J. Biol. Chem.* **276,** 206–214
36. Patterson, J., Palombella, V. J., Fritz, C., and Normant, E. (2008) IPI-504, a novel and soluble HSP-90 inhibitor, blocks the unfolded protein response in multiple myeloma cells. *Cancer Chemother. Pharmacol.* **61,** 923–932
37. Shaffer, A. L., Shapiro-Shelef, M., Iwakoshi, N. N., Lee, A. H., Qian, S. B., Zhao, H., Yu, X., Yang, L., Tan, B. K., Rosenwald, A., Hurt, E. M., Petroulakis, E., Sonenberg, N., Yewdell, J. W., Calame, K., Glimcher, L. H., and Staudt, L. M. (2004) XBP1, downstream of Blimp-1, expands the secretory apparatus and other organelles, and increases protein synthesis in plasma cell differentiation. *Immunity* **21,** 81–93
38. Péterfi, Z., Donkó, A., Orient, A., Sum, A., Prókai, A., Molnár, B., Veréb, Z., Rajnavölgyi, E., Kovács, K. J., Müller, V., Szabó, A. J., and Geiszt, M. (2009) Peroxidasin is secreted and incorporated into the extracellular matrix of myofibroblasts and fibrotic kidney. *Am. J. Pathol.* **175,** 725–735
39. Mackenzie, B., and Erickson, J. D. (2004) Sodium-coupled neutral amino acid (System N/A) transporters of the SLC38 gene family. *Pflugers Arch.* **447,** 784–795
40. Hotamisligil, G. S., and Erbay, E. (2008) Nutrient sensing and inflammation in metabolic diseases. *Nat. Rev. Immunol.* **8,** 923–934
41. Gazzola, R. F., Sala, R., Bussolati, O., Visigalli, R., Dall'Asta, V., Ganapathy, V., and Gazzola, G. C. (2001) The adaptive regulation of amino acid transport system A is associated to changes in ATA2 expression. *FEBS Lett.* **490,** 11–14
42. Alfieri, R. R., Petronini, P. G., Bonelli, M. A., Caccamo, A. E., Cavazzoni, A., Borghetti, A. F., and Wheeler, K. P. (2001) Osmotic regulation of ATA2 mRNA expression and amino acid transport System A activity. *Biochem. Biophys. Res. Commun.* **283,** 174–178
43. DeBerardinis, R. J., and Cheng, T. (2010) Q's next. The diverse functions of glutamine in metabolism, cell biology, and cancer. *Oncogene* **29,** 313–324
44. Gaccioli, F., Huang, C. C., Wang, C., Bevilacqua, E., Franchi-Gazzola, R., Gazzola, G. C., Bussolati, O., Snider, M. D., and Hatzoglou, M. (2006) Amino acid starvation induces the SNAT2 neutral amino acid transporter by a mechanism that involves eukaryotic initiation factor 2α phosphorylation and cap-independent translation. *J. Biol. Chem.* **281,** 17929–17940
45. McDowell, H. E., Eyers, P. A., and Hundal, H. S. (1998) Regulation of System A amino acid transport in L6 rat skeletal muscle cells by insulin, chemical, and hyperthermic stress. *FEBS Lett.* **441,** 15–19
46. Palii, S. S., Thiaville, M. M., Pan, Y. X., Zhong, C., and Kilberg, M. S. (2006) Characterization of the amino acid response element within the human

sodium-coupled neutral amino acid transporter 2 (SNAT2) System A transporter gene. *Biochem. J.* **395,** 517–527
47. Avruch, J., Long, X., Ortiz-Vega, S., Rapley, J., Papageorgiou, A., and Dai, N. (2009) Amino acid regulation of TOR complex 1. *Am. J. Physiol. Endocrinol. Metab.* **296,** E592–E602
48. Nicklin, P., Bergman, P., Zhang, B., Triantafellow, E., Wang, H., Nyfeler, B., Yang, H., Hild, M., Kung, C., Wilson, C., Myer, V. E., MacKeigan, J. P., Porter, J. A., Wang, Y. K., Cantley, L. C., Finan, P. M., and Murphy, L. O. (2009) Bidirectional transport of amino acids regulates mTOR and autophagy. *Cell* **136,** 521–534
49. Evans, K., Nasim, Z., Brown, J., Butler, H., Kauser, S., Varoqui, H., Erickson, J. D., Herbert, T. P., and Bevington, A. (2007) Acidosis-sensing glutamine pump SNAT2 determines amino acid levels and mammalian target of rapamycin signaling to protein synthesis in L6 muscle cells. *J. Am. Soc. Nephrol.* **18,** 1426–1436
50. Wullschleger, S., Loewith, R., and Hall, M. N. (2006) TOR signaling in growth and metabolism. *Cell* **124,** 471–484
51. Ozcan, U., Ozcan, L., Yilmaz, E., Düvel, K., Sahin, M., Manning, B. D., and Hotamisligil, G. S. (2008) Loss of the tuberous sclerosis complex tumor suppressors triggers the unfolded protein response to regulate insulin signaling and apoptosis. *Mol. Cell* **29,** 541–551
52. Baird, F. E., Bett, K. J., MacLean, C., Tee, A. R., Hundal, H. S., and Taylor, P. M. (2009) Tertiary active transport of amino acids reconstituted by coexpression of System A and L transporters in *Xenopus* oocytes. *Am. J. Physiol. Endocrinol. Metab.* **297,** E822–E829
53. Hara, K., Yonezawa, K., Weng, Q. P., Kozlowski, M. T., Belham, C., and Avruch, J. (1998) Amino acid sufficiency and mTOR regulate p70 S6 kinase and eIF-4E BP1 through a common effector mechanism. *J. Biol. Chem.* **273,** 14484–14494
54. Yanagida, O., Kanai, Y., Chairoungdua, A., Kim, D. K., Segawa, H., Nii, T., Cha, S. H., Matsuo, H., Fukushima, J., Fukasawa, Y., Tani, Y., Taketani, Y., Uchino, H., Kim, J. Y., Inatomi, J., Okayasu, I., Miyamoto, K., Takeda, E., Goya, T., and Endou, H. (2001) Human L-type amino acid transporter 1 (LAT1). Characterization of function and expression in tumor cell lines. *Biochim. Biophys. Acta* **1514,** 291–302
55. Walton, F. S., Harmon, A. W., Paul, D. S., Drobná, Z., Patel, Y. M., and Styblo, M. (2004) Inhibition of insulin-dependent glucose uptake by trivalent arsenicals. Possible mechanism of arsenic-induced diabetes. *Toxicol. Appl. Pharmacol.* **198,** 424–433
56. Gjymishka, A., Palii, S. S., Shan, J., and Kilberg, M. S. (2008) Despite increased ATF4 binding at the C/EBP-ATF composite site following activation of the unfolded protein response, system A transporter 2 (SNAT2) transcription activity is repressed in HepG2 cells. *J. Biol. Chem.* **283,** 27736–27747
57. Jung, D. K., Bae, G. U., Kim, Y. K., Han, S. H., Choi, W. S., Kang, H., Seo, D. W., Lee, H. Y., Cho, E. J., Lee, H. W., and Han, J. W. (2003) Hydrogen peroxide mediates arsenite activation of $p70^{s6k}$ and extracellular signal-regulated kinase. *Exp. Cell Res.* **290,** 144–154
58. Wang, X., and Proud, C. G. (1997) p70 S6 kinase is activated by sodium arsenite in adult rat cardiomyocytes. Roles for phosphatidylinositol 3-kinase and p38 MAP kinase. *Biochem. Biophys. Res. Commun.* **238,** 207–212
59. Wu, X. N., Wang, X. K., Wu, S. Q., Lu, J., Zheng, M., Wang, Y. H., Zhou, H., Zhang, H., and Han, J. (2011) Phosphorylation of Raptor by p38β participates in arsenite-induced mammalian target of rapamycin complex 1 (mTORC1) activation. *J. Biol. Chem.* **286,** 31501–31511
60. McGivan, J. D., and Bungard, C. I. (2007) The transport of glutamine into mammalian cells. *Front. Biosci.* **12,** 874–882
61. Barber, E. F., Handlogten, M. E., Vida, T. A., and Kilberg, M. S. (1982) Neutral amino acid transport in hepatocytes isolated from streptozotocin-induced diabetic rats. *J. Biol. Chem.* **257,** 14960–14967
62. Varoqui, H., and Erickson, J. D. (2002) Selective up-regulation of system A transporter mRNA in diabetic liver. *Biochem. Biophys. Res. Commun.* **290,** 903–908
63. Cullinan, S. B., and Diehl, J. A. (2004) PERK-dependent activation of Nrf2 contributes to redox homeostasis and cell survival following endoplasmic reticulum stress. *J. Biol. Chem.* **279,** 20108–20117
64. Fawcett, T. W., Martindale, J. L., Guyton, K. Z., Hai, T., and Holbrook, N. J. (1999) Complexes containing activating transcription factor (ATF)/cAMP-responsive element-binding protein (CREB) interact with the CCAAT/enhancer-binding protein (C/EBP)-ATF composite site to regulate Gadd153 expression during the stress response. *Biochem. J.* **339,** 135–141
65. Guyton, K. Z., Xu, Q., and Holbrook, N. J. (1996) Induction of the mammalian stress response gene GADD153 by oxidative stress. Role of AP-1 element. *Biochem. J.* **314,** 547–554
66. Ma, Y., Brewer, J. W., Diehl, J. A., and Hendershot, L. M. (2002) Two distinct stress signaling pathways converge upon the CHOP promoter during the mammalian unfolded protein response. *J. Mol. Biol.* **318,** 1351–1365